
AUTHOR QUERIES

Journal id: GAPA_A_343064

Corresponding author: Giulio Ciruolo

Title: A method of variation of boundaries for waveguide grating couplers

Dear Author

Please address all the numbered queries on this page which are clearly identified on the proof for your convenience.

Thank you for your cooperation

Query number	Query
1	Please provide Communication details
2	Please mention Figure [1] in the text.
3	Please provide publisher locations.
4	Please provide publisher locations.
5	Have these been published yet? If so, please give details for reference sections.

RESEARCH ARTICLE

A method of variation of boundaries for waveguide grating couplers

Giulio Ciralo*

Dipartimento di Matematica e Applicazioni, Università di Palermo, Palermo, Italy

Communicated by ■■■■

(Received 27 May 2008; final version received 28 July 2008)

We describe a method for calculating the solution of the electromagnetic field in a non-rectilinear open waveguide by using a series expansion, starting from the field of a rectilinear waveguide. Our approach is based on a method of variation of boundaries. We prove that the obtained series expansion converges and we provide a radiation condition at infinity in such a way that the problem has a unique solution. Our approach can model several kinds of optical devices which are used in optical integrated circuits. Numerical examples will be shown for the case of finite aperiodic waveguide grating couplers.

Keywords: wave propagation; Helmholtz equation; optical waveguides

AMS Subject Classifications: 78A40; 78A50; 78M35; 35J05; 35A05

1. Introduction

In recent years, the growing interest in optical integrated circuits stimulated the study of electromagnetic wave propagation in diffraction-dominated structures. The design and use of diffraction-based integrated optics has led to the development of fast and accurate numerical methods for the design of many kinds of optical devices, such as couplers, tapers, gratings, bendings, imperfections of structures and so on.

In a waveguide grating coupler, a guided wave propagating inside the waveguide is coupled to free-space radiation through an *ad hoc* perturbation of the profile of the waveguide (that makes possible to excite a guided wave by illuminating the waveguide by a radiation external to the waveguide). This phenomenon is due to the fact that, since the waveguide is not rectilinear, a pure guided wave is not supported by the waveguide and then the other supported guided waves (if any) and the free-space radiation appear.

Many numerical methods have been proposed for analyzing such structures [1–5]. In the present article we shall propose a rigorous treatment of a method of boundary variation for waveguide problems. Our approach is strictly connected to the method of boundary variation introduced in [6–8] (see also [9–11]), where the authors established that solutions to problems of diffraction of light in a periodic structure behave analytically with respect to variations of the interface. Starting from such results, in [1–5] the authors

*Email: ciralo@math.unifi.it

analysed infinite periodic and finite aperiodic waveguide grating couplers by using an approximate version of the method of boundary variation. In the present article we provide a rigorous approach of the method of boundary variation which allows us to study problems arising from the study of optical devices. Even if our approach applies to a wider class of problems, we shall focus our attention on finite aperiodic waveguide grating couplers, i.e. structures of finite extent (Figure 2).

As it will be clear, our method is applicable whenever it is possible to find a change of coordinates such that the non-rectilinear waveguide is mapped into a rectilinear one. We wish to observe that our method provides a rigorous analysis of finite grating couplers, since it takes into account the coupling between both guided modes and the free-space radiation. Crucial to our approach are the results contained in [12–14]. In [12] the authors found a Green's function for the wave propagation problem in a 2D rectilinear waveguide. The uniqueness of such a problem was studied in [14], where a Rellich type radiation condition at infinity was introduced. Thus, [12] and [14] together provide the knowledge of the only solution for the 2D rectilinear waveguide problem which satisfies a Rellich type radiation condition at infinity. In [13], it was proven the existence of a solution for the perturbed problem. In particular, that was made by showing that the linearized operator is continuous. The main results from [12] and [13] are recalled in Section 2; the ones in [14] are reported in Section 3, where we also generalize such uniqueness result to the case of a non-rectilinear waveguide.

In Section 4 we shall describe our mathematical framework. The adopted method of boundary variation is described in Section 4.1. The analyticity of the solution with respect to the variation of the boundary of the waveguide is proven in Section 4.2.

In Section 5 we apply our analytical results for studying finite aperiodic gratings by showing some numerical examples.

2. Preliminaries

In this section we recall the expression of the Green's formula obtained by Magnanini and Santosa in [12] and the main result in [13].

Our starting point is the Helmholtz equation:

$$\Delta u + k^2 n_0(x)^2 u = f, \quad (x, z) \in \mathbb{R}^2, \quad (1)$$

where k is the wavenumber and the index of refraction n_0 is of the form

$$n_0 := \begin{cases} n_{co}(x), & |x| \leq h, \\ n_{cl}, & |x| > h; \end{cases} \quad (2)$$

here, $n_{co}(\cdot)$ is a bounded function depending only on the transversal coordinate x and $2h$ is the width of the waveguide. Under the *weakly guided approximation* [15] and with such a choice of n , (1) describes the electromagnetic wave propagation in a rectilinear open waveguide with axis along the z -direction.

In [12], the authors look for solutions of the homogeneous equation associated to (1) in the form $u(x, z) = v(x, \lambda) e^{ik\beta z}$; here, $v(x, \lambda)$ satisfies the associated eigenvalue problem for v :

$$v'' + [\lambda - q(x)]v = 0, \quad \text{in } \mathbb{R}, \quad (3)$$

with

$$n_* = \max_{\mathbb{R}} n_0, \quad \lambda = k^2(n_*^2 - \beta^2), \quad q(x) = k^2[n_*^2 - n_0(x)^2]. \quad (4)$$

80 The solutions of (3) can be written in the following form:

$$v_j(x, \lambda) = \begin{cases} \phi_j(h, \lambda) \cos Q(x-h) + \frac{\phi_j'(h, \lambda)}{Q} \sin Q(x-h), & \text{if } x > h, \\ \phi_j(x, \lambda), & \text{if } |x| \leq h, \\ \phi_j(-h, \lambda) \cos Q(x+h) + \frac{\phi_j'(-h, \lambda)}{Q} \sin Q(x+h), & \text{if } x < -h, \end{cases} \quad (5)$$

for $j=s, a$, with $Q = \sqrt{\lambda - d^2}$, $d^2 = k^2(n_*^2 - n_{cl}^2)$ and where the ϕ_j 's are solutions of (3) in the interval $(-h, h)$ and satisfy the following conditions:

$$\begin{aligned} \phi_s(0, \lambda) &= 1, & \phi_s'(0, \lambda) &= 0, \\ \phi_a(0, \lambda) &= 0, & \phi_a'(0, \lambda) &= \sqrt{\lambda}. \end{aligned} \quad (6)$$

85 The indices $j=s, a$ correspond to symmetric and antisymmetric solutions, respectively.

For $0 < \lambda < d^2$, it exists a finite number of eigenvalues (corresponding to the *guided modes*) λ_m^j , $m=1, \dots, M_j$, $j \in \{s, a\}$, satisfying the equations

$$\sqrt{d^2 - \lambda} \phi_j(h, \lambda) + \phi_j'(h, \lambda) = 0, \quad j \in \{s, a\},$$

and corresponding eigenfunctions $v_j(x, \lambda_m^j)$ which satisfy (3). In this case, $v_j(x, \lambda_m^j)$ decays exponentially for $|x| > h$:

90

$$v_j(x, \lambda_m^j) = \begin{cases} \phi_j(h, \lambda_m^j) e^{-\sqrt{d^2 - \lambda_m^j}(x-h)}, & x > h, \\ \phi_j(x, \lambda_m^j), & |x| \leq h, \\ \phi_j(-h, \lambda_m^j) e^{\sqrt{d^2 - \lambda_m^j}(x+h)}, & x < -h. \end{cases} \quad (7)$$

For $\lambda > d^2$, the spectrum is continuous and corresponds to *radiation* and *evanescent modes*. The resulting solution u of (1) has the following form:

$$u(x, z) = \int_{\mathbb{R}^2} G(x, z; \xi, \zeta) f(\xi, \zeta) d\xi d\zeta, \quad (x, z) \in \mathbb{R}^2, \quad (8)$$

95 where the Green's function G is a superposition of guided, radiation and evanescent modes:

$$G(x, z; \xi, \zeta) = \sum_{j \in \{s, a\}} \int_0^{+\infty} \frac{e^{i|z-\zeta|\sqrt{k^2 n_*^2 - \lambda}}}{2i\sqrt{k^2 n_*^2 - \lambda}} v_j(x, \lambda) v_j(\xi, \lambda) d\rho_j(\lambda), \quad (9)$$

with

$$\langle d\rho_j, \eta \rangle = \sum_{m=1}^{M_j} r_m^j \eta(\lambda_m^j) + \frac{1}{2\pi} \int_{d^2}^{+\infty} \frac{\sqrt{\lambda - d^2}}{(\lambda - d^2)\phi_j(h, \lambda)^2 + \phi_j'(h, \lambda)^2} \eta(\lambda) d\lambda,$$

100 for all $\eta \in C_0^\infty(\mathbb{R})$, where

$$r_m^j = \left[\int_{-\infty}^{+\infty} v_j(x, \lambda_m^j)^2 dx \right]^{-1} = \frac{\sqrt{d^2 - \lambda_m^j}}{\sqrt{d^2 - \lambda_m^j} \int_{-h}^h \phi_j(x, \lambda_m^j)^2 dx + \phi_j(h, \lambda_m^j)^2}.$$

We notice that (9) can be split up into three summands $G = G^g + G^r + G^e$, where

$$G^g(x, z; \xi, \zeta) = \sum_{j \in \{s, a\}} \sum_{m=1}^{M_j} \frac{e^{i|z-\zeta|\sqrt{k^2 n_*^2 - \lambda_m^j}}}{2i\sqrt{k^2 n_*^2 - \lambda_m^j}} v_j(x, \lambda_m^j) v_j(\xi, \lambda_m^j) r_m^j, \quad (10a)$$

$$G^r(x, z; \xi, \zeta) = \frac{1}{2\pi} \sum_{j \in \{s, a\}} \int_{d^2}^{k^2 n_*^2} \frac{e^{i|z-\zeta|\sqrt{k^2 n_*^2 - \lambda}}}{2i\sqrt{k^2 n_*^2 - \lambda}} v_j(x, \lambda) v_j(\xi, \lambda) \sigma_j(\lambda) d\lambda, \quad (10b)$$

$$G^e(x, z; \xi, \zeta) = -\frac{1}{2\pi} \sum_{j \in \{s, a\}} \int_{k^2 n_*^2}^{+\infty} \frac{e^{-|z-\zeta|\sqrt{\lambda - k^2 n_*^2}}}{2\sqrt{\lambda - k^2 n_*^2}} v_j(x, \lambda) v_j(\xi, \lambda) \sigma_j(\lambda) d\lambda, \quad (10c)$$

with

$$\sigma_j(\lambda) = \frac{\sqrt{\lambda - d^2}}{(\lambda - d^2)\phi_j(h, \lambda)^2 + \phi_j'(h, \lambda)^2}. \quad (11)$$

105 G^g represents the guided part of the Green's function, which describes the guided modes, i.e. the modes propagating mostly inside the core; G^r and G^e are the parts of the Green's function corresponding to the radiation and evanescent modes, respectively. The radiation and evanescent components altogether form the radiating part G^{rad} of G

$$G^{\text{rad}} = G^r + G^e = \frac{1}{2\pi} \sum_{j \in \{s, a\}} \int_{d^2}^{+\infty} \frac{e^{i|z-\zeta|\sqrt{k^2 n_*^2 - \lambda}}}{2i\sqrt{k^2 n_*^2 - \lambda}} v_j(x, \lambda) v_j(\xi, \lambda) \sigma_j(\lambda) d\lambda, \quad (12)$$

110 and the corresponding radiating part of the solution

$$u^{\text{rad}}(x, z) = \int_{\mathbb{R}^2} G^{\text{rad}}(x, z; \xi, \zeta) f(\xi, \zeta) d\xi d\zeta. \quad (13)$$

The main results in [13] was to bound an inverse of the Helmholtz operator. Since we are dealing with unbounded domains, we shall introduce weighted Sobolev spaces. 115 Let $\mu : \mathbb{R}^2 \rightarrow \mathbb{R}$ be a positive function such that $|\mu| \leq 1$ and

$$\mu \in C^2(\mathbb{R}^N) \cap L^1(\mathbb{R}^N), \quad |\nabla \mu| \leq C_1 \mu, \quad |\nabla^2 \mu| \leq C_2 \mu, \quad \text{in } \mathbb{R}^N, \quad (14)$$

where C_1 and C_2 are positive constants; for instance

$$\mu = (1 + |x|^2 + |z|^2)^{-\tau}, \quad (15)$$

120 $\tau > 1$, can be a good choice. We will denote by $L^2(\mu)$ the weighted space consisting of all the complex valued measurable functions $u(x, z)$, $(x, z) \in \mathbb{R}^2$, such that $\mu^{\frac{1}{2}} u \in L^2(\mathbb{R}^2)$, equipped with the natural norm

$$\|u\|_{L^2(\mu)}^2 = \int_{\mathbb{R}^2} |u(x, z)|^2 \mu(x, z) dx dz.$$

In a similar way we define the weighted Sobolev spaces $H^1(\mu)$ and $H^2(\mu)$.

The following theorem was proved in [13]:

125 **THEOREM 2.1** *Let u be the solution of (1) given by (8). Then*

$$\|u\|_{H^2(\mu)} \leq C_0 \|f\|_{L^2(\mu^{-1})}, \tag{16}$$

where

$$C_0^2 = \frac{5}{2} + 2C_2 + \left[\frac{3}{2} + 4C_2 + 8C_2^2 + (1 + 4C_2)k^2n_*^2 + 2k^4n_*^4 \right] \|G\|_{L^2(\mu \times \mu)}^2, \tag{17}$$

where C_2 is defined by (14).

130 **3. Uniqueness of solutions**

In [14], it was proved that (8) is the only solution of (1) satisfying certain radiation conditions at infinity. We recall such a result in the following and then generalize that to the case of non-rectilinear waveguides.

135 Following [14], it will be useful to introduce slightly different notations. We denote by γ_l , $l = 1, \dots, M$, $M = M_s + M_a$, the values λ_m^j , $m = 1, \dots, M_j$, $j = s, a$, and

$$\gamma_* = \max_{l=1, \dots, M} \gamma_l. \tag{18}$$

We set

$$e(x, \gamma_l) = \frac{v_j(x, \gamma_l)}{\|v_j(\cdot, \gamma_l)\|_2}, \tag{19}$$

where we choose v_j , $j \in \{s, a\}$, according to the λ_m^j corresponding to γ_l , and define

$$u^l(x, z) = e(x, \gamma_l)U(z, \gamma_l), \tag{20}$$

140 with

$$U(z, \gamma_l) = \int_{-\infty}^{\infty} u(\xi, z)e(\xi, \gamma_l)d\xi, \quad l = 1, \dots, M, \tag{21}$$

and

$$u^0(x, z) = u(x, z) - \sum_{l=1}^M u^l(x, z). \tag{22}$$

145 Moreover, we set

$$\Omega_\rho = \{(x, z) \in \mathbb{R}^2 : [\max(|x| - h, 0)]^2 + z^2 \leq \rho^2\}, \tag{23}$$

$\beta_0 = kn_{cl}$ and $\beta_l = \sqrt{k^2n_*^2 - \gamma_l}$, for $l = 1, \dots, M$.

The main results in [13] are collected in the following theorem.

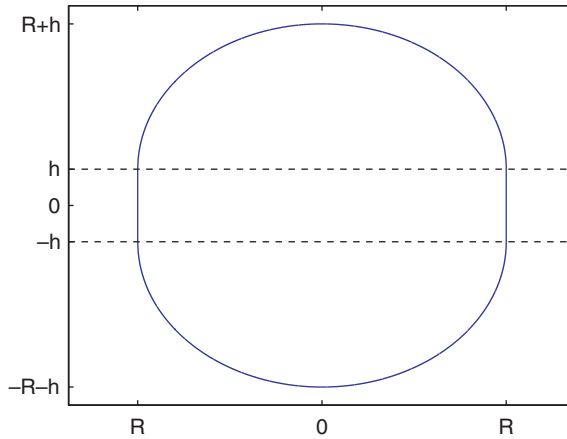


Figure 1. The set Ω_R .

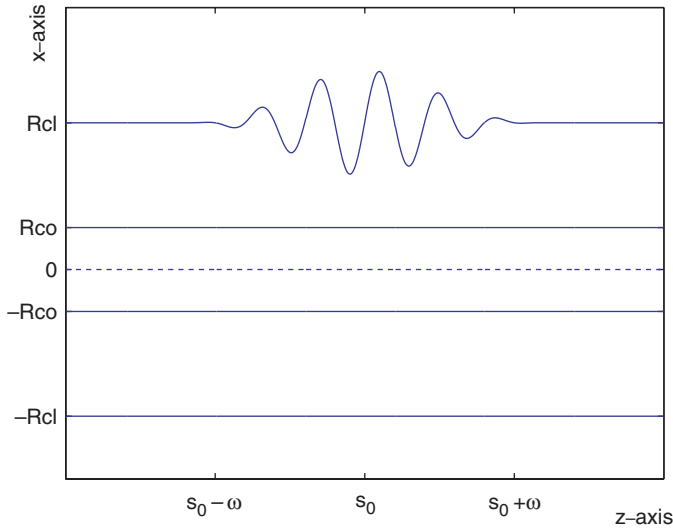


Figure 2. The profile of the perturbed waveguide. This example models a finite aperiodic grating coupler.

150 **THEOREM 3.1** *Let u be the solution of (1) defined by (8). Then u is the only solution of (1) such that $u \in L^2(\mu)$ and*

$$\sum_{l=0}^M \int_0^\infty \int_{\partial\Omega_\rho} \left| \frac{\partial u^l}{\partial \nu} - i\beta_l u^l \right|^2 d\ell d\rho < +\infty, \quad (24)$$

where ν denotes the outward normal to the set $\partial\Omega_\rho$.

In this section we shall prove an analogous result for the non-rectilinear problem

$$L_\varepsilon u := \Delta u + k^2 n_\varepsilon(x, z)^2 u = f, \quad (x, z) \in \mathbb{R}^2, \quad (25)$$

155 where n_ε is a perturbation of the function n_0 defined by (2). In particular, we assume that $n_\varepsilon - n_0$ is a compactly supported function, i.e.

$$\text{supp}(n_\varepsilon - n_0) \subset \Omega_{\rho_0}, \tag{26}$$

for some $\rho_0 > 0$, and prove that it exists a unique solution of (25) which satisfies (24). In order to do that, we shall adapt the proofs of Lemma 2.5 and Theorems 2.6 and 2.7 in [14] to this case.

160

LEMMA 3.2 *Let $\beta \in \mathbb{R}$ and $n_\varepsilon \in L^\infty(\mathbb{R}^2)$. If u is a weak solution of*

$$\Delta u + k^2 n_\varepsilon(x, z)^2 u = 0, \tag{27}$$

then

$$\text{Im} \int_{\partial D} \bar{u} \frac{\partial u}{\partial \nu} d\sigma = 0,$$

165 i.e.

$$\int_{\partial D} \left| \frac{\partial u}{\partial \nu} - i\beta u \right|^2 d\sigma = \int_{\partial D} \left(\left| \frac{\partial u}{\partial \nu} \right|^2 + \beta^2 |u|^2 \right) d\sigma, \tag{28}$$

for every $\Omega \subset \mathbb{R}^2$ bounded and sufficiently smooth.

The proof of this lemma is omitted, because it is analogous to the one done for Lemma 2.5 in [14].

170

We introduce the following notations, which will be useful throughout the present section:

$$S = \{(x, z) \in \mathbb{R}^2 : |z| \leq \rho_0\}, \quad \Omega_\rho^I = \Omega_\rho \cap S, \quad \Omega_\rho^E = \Omega_\rho \cap (\mathbb{R}^2 \setminus S), \tag{29}$$

for $\rho > \rho_0$, and set

$$\partial\Omega_\rho^I = \partial_S\Omega_\rho^I \cup \partial_e\Omega_\rho^I, \quad \partial\Omega_\rho^E = \partial_S\Omega_\rho^E \cup \partial_e\Omega_\rho^E,$$

175

where $\partial_S\Omega_\rho^I$ and $\partial_e\Omega_\rho^I$ are the portions of $\partial\Omega_\rho^I$ laying on ∂S and $\partial\Omega_\rho$, respectively; analogously we define $\partial_S\Omega_\rho^E$ and $\partial_e\Omega_\rho^E$ and notice that

$$\partial\Omega_\rho = \partial_e\Omega_\rho^I \cup \partial_e\Omega_\rho^E. \tag{30}$$

For the sake of simplicity, we shall assume that μ is as in (15). Analogous results hold for more general μ satisfying (14).

180

LEMMA 3.3 *Let $u \in L^2(\mu)$ be a solution of (27). Then*

$$u - u^0 = \mathcal{O}(e(x, \gamma_*)), \quad |\nabla u - \nabla u^0| = \mathcal{O}(e(x, \gamma_*)), \tag{31}$$

uniformly as $|x| \rightarrow +\infty$ for $z \in \mathbb{R}$, where u^0 , $e(x, \gamma_*)$ and γ_* are defined by (22), (19) and (18), respectively.

Proof From (22) we need to prove that u_l , $|\nabla u_l| = \mathcal{O}(e(x, \gamma_*))$, uniformly as $|x| \rightarrow +\infty$ for $z \in \mathbb{R}$, for each $l = 1, \dots, M$. From (20) and (27) we have that $U(z, \gamma_l)$ satisfies

185

$$U''(z, \gamma_l) + (k^2 n_*^2 - \gamma_l)U(z, \gamma_l) = g(z),$$

with

$$g(z) = \int_{\mathbb{R}} [n_0(\xi) - n_\varepsilon(\xi, z)] u(\xi, z) e(\xi, \gamma_l) d\xi,$$

and thus

$$U(z, \gamma_l) = \left[c_1 - \frac{i}{2\gamma_l} \int_{\mathbb{R}} g(\zeta) e^{-i\gamma_l \zeta} d\zeta \right] e^{i\gamma_l z} + \left[c_2 + \frac{i}{2\gamma_l} \int_{\mathbb{R}} g(\zeta) e^{i\gamma_l \zeta} d\zeta \right] e^{-i\gamma_l z},$$

190 for some constants c_1 and c_2 . We notice that $u \in H_{\text{loc}}^2(\mathbb{R}^2)$ (see Theorem 8.8 in [16]) and thus, by Sobolev Embedding Theorem [17], u is bounded on every compact subset of \mathbb{R}^2 . Since the support of $n_\varepsilon - n_0$ is contained in Ω_{ρ_0} , we have

$$|U(z, \gamma_l)| \leq |c_1| + |c_2| + \frac{e_* \|n_\varepsilon - n_0\|_1}{\gamma_l} \max_{(x,z) \in \Omega_{\rho_0}} |u(x, z)|,$$

195 and

$$|U'(z, \gamma_l)| \leq \gamma_l (|c_1| + |c_2|) + e_* \|n_\varepsilon - n_0\|_1 \max_{(x,z) \in \Omega_{\rho_0}} |u(x, z)|,$$

where

$$e_* = \max_{l=1, \dots, M} \|e(\cdot, \gamma_l)\|_\infty.$$

200 Thus, since $e(x, \gamma_l)$ and $e'(x, \gamma_l)$ are $\mathcal{O}(e(x, \gamma_*))$ as $|x| \rightarrow +\infty$, from (20) and (22) we obtain (31). ■

Now, we derive some asymptotic formulas which will be useful for proving the next theorem.

By following the proof of Lemma 2.3 in [14], it is easy to show that

$$\|u\mu^{\frac{1}{2}}\|_{L^\infty(S)} \|\mu^{\frac{1}{2}} \nabla u\|_{L^\infty(S)} < +\infty, \tag{32}$$

205 where S is given by (29). Let $\omega: [0, +\infty) \rightarrow \mathbb{R}$ be the function defined by

$$\omega(\rho) = (1 + \rho^2)^\tau e(\rho, \gamma_*), \tag{33}$$

with $\tau > 1$ (notice that ω is a C^1 function and, furthermore, $\omega \in L^\infty(\mathbb{R}^+) \cap L^1(\mathbb{R}^+)$). By using (31) and (32), it is easy to prove the following asymptotic relations that hold uniformly as $\rho \rightarrow +\infty$:

$$\int_{\partial_\varepsilon \Omega'_\rho} \left| \frac{\partial u}{\partial v} - i\beta_0 u \right|^2 d\ell - \int_{\partial_\varepsilon \Omega'_\rho} \left| \frac{\partial u^0}{\partial v} - i\beta_0 u^0 \right|^2 d\ell = \mathcal{O}(\omega(\rho)), \tag{34a}$$

$$\int_{\partial_\varepsilon \Omega'_\rho} \left(\left| \frac{\partial u}{\partial v} \right|^2 + \beta_0^2 |u|^2 \right) d\ell - \int_{\partial_\varepsilon \Omega'_\rho} \left(\left| \frac{\partial u^0}{\partial v} \right|^2 + \beta_0^2 |u^0|^2 \right) d\ell = \mathcal{O}(\omega(\rho)), \tag{34b}$$

$$\text{Im} \int_{\partial_S \Omega'_\rho} \bar{u} \frac{\partial u}{\partial v} d\ell - \text{Im} \int_{\partial_S \Omega'_\rho} \bar{u}^0 \frac{\partial u^0}{\partial v} d\ell = \mathcal{O}(\omega(\rho)). \tag{34c}$$

210 Moreover, from (7), we have

$$\int_{\partial_c \Omega'_\rho} \left(\left| \frac{\partial u^l}{\partial v} \right|^2 + \beta_0^2 |u^l|^2 \right) d\ell = \mathcal{O}(e(\rho, \gamma_*)^2), \tag{35a}$$

$$\text{Im} \int_{\partial_S \Omega'_\rho} \bar{u}^l \frac{\partial u^l}{\partial v} d\ell = \mathcal{O}(e(\rho, \gamma_*)^2), \tag{35b}$$

for $l = 1, \dots, M$, as $\rho \rightarrow \infty$.

215 **THEOREM 3.4** Let $u \in L^2(\mu)$ be a weak solution of (27), with $n_\varepsilon \in L^\infty(\mathbb{R}^2)$ as in (26), and assume that u satisfies (24). Let

$$J(\rho) = \sum_{l=0}^M \int_{\partial \Omega_\rho} \left[\left| \frac{\partial u^l}{\partial v} \right|^2 + \beta_l^2 |u^l|^2 \right] d\ell; \tag{36}$$

then

$$\int_0^{+\infty} J(\rho) d\rho < +\infty, \tag{37}$$

and, in particular,

$$\int_{\mathbb{R}^2} |u^l|^2 dx dz < +\infty, \tag{38}$$

220 for every $l = 0, 1, 2, \dots, M$.

Proof In this proof, we will make use of Lemma 3.2. We notice that we can apply Lemma 3.2 to u and to any set Ω (in particular Ω_ρ^I). The same does not hold for u_l , $l = 0, 1, \dots, M$; in this case, u_l , $l = 0, 1, \dots, M$, is solution of (27) in Ω_ρ^E , for $\rho > \rho_0$, (Theorem 2.6 in [14]) and thus we can apply Lemma 3.2 to u_l , $l = 0, 1, \dots, M$, and by using $\Omega = \Omega_\rho^E$.

From (30), (34b) and (35a) it follows that

$$J(\rho) = \int_{\partial_c \Omega'_\rho} \left(\left| \frac{\partial u}{\partial v} \right|^2 + \beta_0^2 |u|^2 \right) d\ell + \sum_{l=0}^M \int_{\partial_c \Omega_\rho^E} \left(\left| \frac{\partial u^l}{\partial v} \right|^2 + \beta_l^2 |u^l|^2 \right) d\ell + \mathcal{O}(\omega(\rho)),$$

230 uniformly as $\rho \rightarrow +\infty$. Since $n_\varepsilon \equiv n_0$ in $\mathbb{R}^2 \setminus \Omega_{\rho_0}$, each u^l , $l = 0, 1, \dots, M$, is a weak solution of (27) in Ω_ρ^E , for $\rho > \rho_0$ (Theorem 2.6 in [14]). Thus, from the above equation and by applying Lemma 3.2 to u and u^l , $l = 0, 1, \dots, M$, in Ω_ρ^I and Ω_ρ^E , respectively, we obtain

$$\begin{aligned} J(\rho) &= \int_{\partial_c \Omega'_\rho} \left| \frac{\partial u}{\partial v} - i\beta_0 u \right|^2 d\ell - \int_{\partial_S \Omega'_\rho} \left(\left| \frac{\partial u}{\partial v} \right|^2 + \beta_0^2 |u|^2 \right) d\ell + \sum_{l=0}^M \int_{\partial_c \Omega_\rho^E} \left| \frac{\partial u^l}{\partial v} - i\beta_l u^l \right|^2 d\ell \\ &\quad - \sum_{l=0}^M \int_{\partial_S \Omega_\rho^E} \left(\left| \frac{\partial u^l}{\partial v} \right|^2 + \beta_l^2 |u^l|^2 \right) d\ell + \mathcal{O}(\omega(\rho)) \\ &= \int_{\partial_c \Omega'_\rho} \left| \frac{\partial u}{\partial v} - i\beta_0 u \right|^2 d\ell - 2\beta_0 \int_{\partial_S \Omega'_\rho} \text{Im} \bar{u} \frac{\partial u}{\partial v} d\ell + \sum_{l=0}^M \int_{\partial_c \Omega_\rho^E} \left| \frac{\partial u^l}{\partial v} - i\beta_l u^l \right|^2 d\ell \\ &\quad - \sum_{l=0}^M 2\beta_l \int_{\partial_S \Omega_\rho^E} \text{Im} \bar{u}_l \frac{\partial u^l}{\partial v} d\ell + \mathcal{O}(\omega(\rho)), \end{aligned}$$

as $\rho \rightarrow +\infty$, and, from (34a), we have

$$J(\rho) = \int_{\partial_\varepsilon \Omega'_\rho} \left| \frac{\partial u^0}{\partial \nu} - i\beta_0 u^0 \right|^2 d\ell + \sum_{l=0}^M \int_{\partial_\varepsilon \Omega_\rho^E} \left| \frac{\partial u^l}{\partial \nu} - i\beta_l u^l \right|^2 d\ell - 2\beta_0 \int_{\partial_S \Omega'_\rho} \operatorname{Im} \bar{u}_0 \frac{\partial u^0}{\partial \nu} d\ell - \sum_{l=0}^M 2\beta_l \int_{\partial_S \Omega_\rho^E} \operatorname{Im} \bar{u}_l \frac{\partial u^l}{\partial \nu} d\ell + \mathcal{O}(\omega(\rho)),$$

235 as $\rho \rightarrow +\infty$. By adding

$$\sum_{l=1}^M \int_{\partial_\varepsilon \Omega'_\rho} \left| \frac{\partial u^l}{\partial \nu} - i\beta_l u^l \right|^2 d\ell$$

to the above equation and since

$$\int_{\partial_S \Omega'_\rho} + \int_{\partial_S \Omega_\rho^E} \operatorname{Im} \bar{u}_0 \frac{\partial u^0}{\partial \nu} d\ell = 0,$$

from (30) and (35b), we get

$$J(\rho) \leq \sum_{l=0}^M \int_{\Omega_\rho} \left| \frac{\partial u^l}{\partial \nu} - i\beta_l u^l \right|^2 d\ell + \mathcal{O}(\omega(\rho)),$$

240 as $\rho \rightarrow +\infty$. From (24) and since $\omega(\cdot), e(\cdot, \gamma_*)^2 \in L^1(\mathbb{R}^+)$, we obtain (37) and (38). ■

The uniqueness theorem for (25) is the following:

THEOREM 3.5 *Let n_ε satisfy (26). There exists at most one weak solution $u \in L^2(\mu)$ of (25) which satisfies (24).*

245 Since n_ε coincides with n_0 outside a compact set, the proof of Theorem 2.7 in [14] can be easily adapted to prove the above theorem.

4. The method of variation of boundaries

In the present section we propose an analytical approach to the study of non-rectilinear waveguides. We shall study the Helmholtz equation (25) and the corresponding operator
250 $L_\varepsilon = \Delta + k^2 n_\varepsilon(x, z)^2$. Again, we remark that the waveguide is no more rectilinear and thus we are assuming that the index of refraction n depends on both the x - and z -coordinates. In particular, we are interested in perturbations which can be described by a geometric transformation of the plane, in a sense that we are going to explain shortly.

255 Our approach consists in finding a suitable change of coordinates such that, after having changed the coordinates, n_ε depends only on the ‘new’ transversal coordinate or it can be represented in Neumann series with the zeroth order term depending only on the new transversal coordinate. Then, in the new coordinates, we formally represent u and the operator L_ε by their Neumann series:

$$u = u_\varepsilon = u_0 + \varepsilon u_1 + \varepsilon^2 u_2 + \dots, \quad L_\varepsilon = L_0 + \varepsilon L_1 + \varepsilon^2 L_2 + \dots,$$

260 where $\varepsilon > 0$ is supposed to be small. Here, $L_0 = \Delta + k^2 n_0(x)^2$ is the operator corresponding to the Helmholtz equation for the case of a rectilinear waveguide. By using the above

formulas and equating the asymptotic terms of the same order, we can solve $L_\varepsilon u_\varepsilon = f$ by iteration:

$$L_0 u_0 = f, \quad L_0 u_1 = -L_1 u_0, \dots, L_0 u_N = -\sum_{j=0}^{N-1} L_{j+1} u_{N-1-j}, \dots \quad (39)$$

265 Each step of (39) can be solved by using (8). Then, we prove that the resulting Neumann series for u converges and, thanks also to the results in the previous section, we have the existence and uniqueness of the solution.

In Section 4.1 we shall give a rigorous treatment of the boundary variation method described above. In Section 4.2 we prove that the iterative procedure (39) leads to
270 a converging series for the solution u .

4.1. A method of variation of boundaries

As already mentioned, our idea is that of transforming a non-rectilinear waveguide into a rectilinear one by a change of variables $\Gamma: \mathbb{R}^2 \rightarrow \mathbb{R}^2$. For this reason, we suppose that Γ is a C^2 invertible function:

$$\Gamma(s, t) = (x(s, t), z(s, t)).$$

275 By setting $w(s, t) = u(x, z)$, a solution u of (1) is converted into a solution w of

$$|\nabla s|^2 w_{ss} + |\nabla t|^2 w_{tt} + 2\nabla s \cdot \nabla t w_{st} + \Delta s \cdot w_s + \Delta t \cdot w_t + c(s, t)^2 w = F(s, t), \quad (40)$$

where $c(s, t) = kn(x(s, t), z(s, t))$ and $F(s, t) = f(x(s, t), z(s, t))$.

For simplicity of exposition, we shall assume that $\Gamma = \Gamma^\varepsilon$ is of the form¹

$$\Gamma^\varepsilon(t, s) = \begin{cases} x = t + \varepsilon\psi(t, s), \\ z = s, \end{cases} \quad (41)$$

280 with

$$\psi(t, s) = T(t)S(s), \quad (42)$$

where $T \in C_c^2(\mathbb{R})$ and $S \in C_c^2(\mathbb{R})$ describes the ‘profile’ of the perturbation, in a sense that we are going to explain shortly. We will explain which roles are played by T and S later.

285 We consider Γ^ε as in (41) and assume that $\psi(t, s)$ is such that $n_\varepsilon(\Gamma^\varepsilon(t, s)) = n_0(t)$. By changing the coordinates and using (40), the operator L_ε in (25) becomes

$$\begin{aligned} L^\varepsilon w := & \frac{1 + \varepsilon^2 \psi_s^2}{(1 + \varepsilon \psi_t)^2} w_{tt} - 2 \frac{\varepsilon \psi_s}{1 + \varepsilon \psi_t} w_{ts} + w_{ss} \\ & - \frac{1}{(1 + \varepsilon \psi_t)^3} [\varepsilon(1 + \varepsilon^2 \psi_s^2) \psi_{tt} - 2\varepsilon^2(1 + \varepsilon \psi_t) \psi_s \psi_{st} + \varepsilon(1 + \varepsilon \psi_t)^2 \psi_{ss}] w_t \\ & + k^2 n_0 \varepsilon(t)^2 w = \tilde{f}(t, s), \quad (t, s) \in \mathbb{R}^2, \end{aligned} \quad (43)$$

with $\tilde{f}(t, s) = f(x, z)$, $w(t, s) = u(x, z)$. Again, we stress the fact that Γ^ε is chosen in such a way that the new refraction coefficient in (43) is $n_0(t)$, where n_0 is the function defined
290 by (2) that models a rectilinear waveguide. More general functions Γ can be considered, but we will restrict to the simpler and significative one introduced above.

The smoothness assumption on S and T makes the coefficients of L^ε continuous. By choosing S compactly supported we suppose that the waveguide is rectilinear outside a bounded region of the plane, that is $L^\varepsilon = L^0$ outside a compact set. The function $T(t)$ is introduced in order to make Γ be a smooth and invertible transformation of the plane.

For instance, in the example shown in Figure 2 (a finite aperiodic grating coupler), a good choice of S and T are the ones represented in Figure 3. In Figure 4, we visualize how Γ transforms the plane, by representing in the (x, z) -plane the image of a rectangular grid in the (t, s) -plane.

The parameter ε controls the amplitude of the perturbation (note that when $\varepsilon = 0$ there is no perturbation at all).

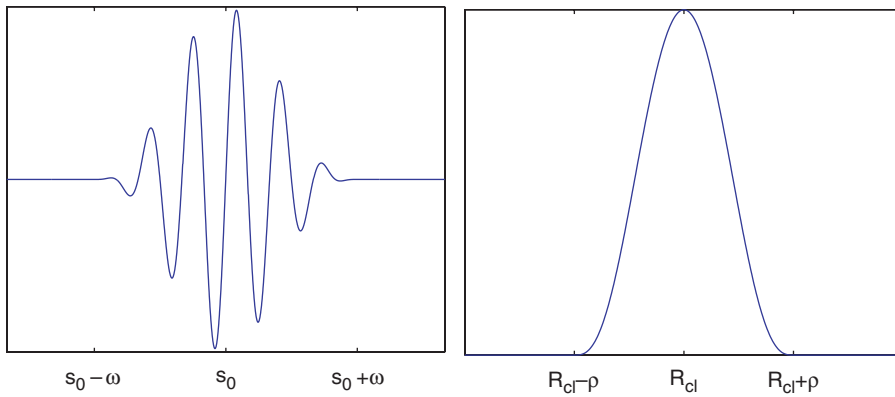


Figure 3. The figures show the choice we made for the functions S and T , respectively. Such a choice corresponds to a perturbed waveguide as in Figure 2.

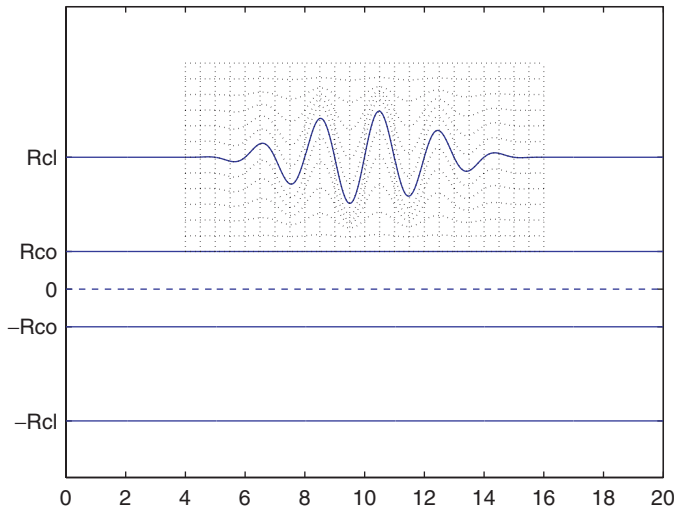


Figure 4. The effect of Γ on the (x, z) -plane. Notice that, with the choice of T as in Figure 3, the perturbed region is bounded.

By expanding w and L^ε by their Neumann series as described before, we find that

$$L_0 w = \Delta w + k^2 n_0(t)^2 w, \tag{44a}$$

$$L_1 w = -2\psi_t w_{tt} - 2\psi_s w_{st} - (\psi_{tt} + \psi_{ss}) w_t, \tag{44b}$$

$$L_2 w = (3\psi_t^2 + \psi_s^2) w_{tt} + 2\psi_s \psi_t w_{st} + (3\psi_{tt} \psi_t + 2\psi_s \psi_{st} + \psi_{ss} \psi_t) w_t, \tag{44c}$$

305 and

$$\begin{aligned} L_j w = & (-1)^j \left\{ \left[(j+1)\psi_t^j + (j-1)\psi_t^{j-2}\psi_s^2 \right] w_{tt} + 2\psi_s \psi_t^{j-1} w_{st} \right. \\ & \left. + \frac{1}{2} \left[(j+1)j\psi_t^{j-1}\psi_{tt} + (j-1)(j-2)\psi_t^{j-3}\psi_s^2\psi_{tt} + 4(j-1)\psi_t^{j-2}\psi_s\psi_{st} + 2\psi_t^{j-1}\psi_{ss} \right] w_t \right\}, \end{aligned} \tag{44d}$$

for $j \geq 3$. Thus, by (39), w can be found by solving

$$\begin{cases} L_0 w_N = F_N, \\ w_N \text{ satisfies (24),} \end{cases} \tag{45}$$

where we set $F_0 = \tilde{f}$ and

$$F_N = \sum_{j=0}^{N-1} L_{j+1} w_{N-1-j}, \quad N \geq 1, \tag{46}$$

310 with $L_j, j \geq 0$, given by (44). We notice that, thanks to Theorem 3.1, each step of the iterative method described by (45) determines a unique solution w_N .

4.2. Analyticity of the solution

315 In this subsection we shall prove that the solution w of (43) given by (45) and (46) is analytic in ε . We shall assume that ψ satisfies the following assumption:

$$|\psi_t|, |\psi_s|, |\psi_{tt}|, |\psi_{ts}|, |\psi_{ss}| \leq K\mu \quad \text{in } \mathbb{R}^2, \tag{47}$$

for some constant K independent of ε . We notice that if $\psi \in C_0^2(\mathbb{R}^2)$, then (47) is satisfied. Before proving the main theorem, we need the following two lemmas, where we prove estimates for the right-hand side of (44) at each step of the inductive procedure.

320 **LEMMA 4.1** *Let L_j be defined by (44) and assume that ψ satisfies (47). Then*

$$\|L_j w\|_{L^2(\mu^{-1})} \leq j(j+1)K^j \|w\|_{H^2(\mu)}, \tag{48}$$

$j \geq 1$, where K is defined by (47).

Proof We notice that, since $0 < \mu \leq 1$, it holds that $\mu^{2j-1} \leq \mu$, for $j \geq 1$. Then, (48) follows easily by applying Minkowski inequality and using (47). ■

325 **LEMMA 4.2** *Let $N \geq 1$ and suppose that*

$$\|w_m\|_{H^2(\mu)} \leq AB^m, \tag{49}$$

for every $m < N$ and for positive constants A and B . Let F_N be defined by (46). If $B > K$, then

$$\|F_N\|_{L^2(\mu^{-1})} \leq 2AK \left(1 - \frac{K}{B}\right)^{-3} B^{N-1}, \tag{50}$$

with K given by (47).

330 *Proof* By Minkowski inequality and Lemma 4.1 we have

$$\begin{aligned} \|F_N\|_{L^2(\mu^{-1})} &\leq \sum_{j=0}^{N-1} \|L_{j+1} w_{N-1-j}\|_{L^2(\mu^{-1})} \\ &\leq \sum_{j=0}^{N-1} (j+1)(j+2)K^{j+1} \|w_{N-1-j}\|_{H^2(\mu)}. \end{aligned}$$

From (49) we get

$$\|F_N\|_{L^2(\mu^{-1})} \leq AKB^{N-1} \sum_{j=0}^{N-1} (j+1)(j+2) \left(\frac{K}{B}\right)^j,$$

and then, since

$$\sum_{k=1}^{\infty} k(k+1)q^k = \frac{2q}{(1-q)^3},$$

335 for $|q| < 1$, (50) follows. ■

THEOREM 4.3 Let $f \in L^2(\mu^{-1})$ and let C_0 be given by (17). If ψ satisfies (47), then it exists a solution

$$w = \sum_{N=0}^{+\infty} w_N \varepsilon^N$$

340 of (40), with w_N , $N=0, 1, \dots$, given by (45), satisfying

$$\|w_N\|_{H^2(\mu)} \leq C_0 \|f\|_{L^2(\mu^{-1})} B^N, \tag{51}$$

for any $\varepsilon < B^{-1}$ and $B > B_0$, where $B_0 > K$ is the solution of

$$B = 2KC_0 \left(1 - \frac{K}{B}\right)^{-3}, \tag{52}$$

with C_0 and K given by (17) and (47), respectively.

345 Moreover, if ψ is compactly supported, w is the only solution of (40) which satisfies (24).

Proof Since each w_N , $N=0, 1, \dots$, satisfies (24), it is clear that, once we have (51), w satisfies (24) and the uniqueness of the solution follows by Theorem 3.1.

To prove (51) we proceed inductively. For $N=0$, (51) follows by Lemma 2.1. Assume that (51) holds for all $j < N$. By applying Lemma 2.1 we have

$$\|w_N\|_{H^2(\mu)} \leq C_0 \|F_N\|_{L^2(\mu^{-1})};$$

350 Lemma 4.2 and the above inequality imply

$$\|u_N\|_{H^2(\mu)} \leq 2C_0^2 \left(1 - \frac{K}{B}\right)^{-3} K \|f\|_{L^2(\mu^{-1})} B^{N-1},$$

and, by choosing $B > \max \{2C_0K(1 - \frac{K}{B})^{-3}, K\}$, we obtain (51). ■

5. Numerical examples

355 In this section, we use the results in Section 4 for studying the wave propagation in presence of finite aperiodic gratings, by showing some numerical results.

Following the scheme described in Section 4.1, we assume that w_0 is a pure guided mode of a rectilinear waveguide, without perturbations. In other words we are taking a special choice of f . Thus, w_0 propagates undisturbed if no imperfections are present.

360 If the waveguide is perturbed, radiating energy together with the remaining guided modes (if any) supported by the waveguide appear. The occurrence of these phenomena will be made clear by pictures presented in this section Figure 5.

We shall assume that the ‘perturbed region’ P is a compact set in \mathbb{R}^2 , as follows from the assumptions on T and S made in Section 4.1. Thus, it is clear that, in such a case, 365 we can apply Theorem 4.3, because the coefficients of L^ε are smooth and with compact support.

In our simulations we compute w_1 : its computation is made easier by the fact that we know the explicit expression of w_0 . The computation of w_2, w_3, \dots would require a larger numerical effort. However, since we know that ε cannot be taken larger than 370 $\varepsilon_0 = B_0^{-1}$, with B_0 given by (52), the contribution of $\varepsilon^2 w_2, \varepsilon^3 w_3, \dots$ would be, generally, rather small.

We consider a 2D waveguide in all its components: a central zone (the core), a finite cladding and then an infinite jacket, see Figure 2.

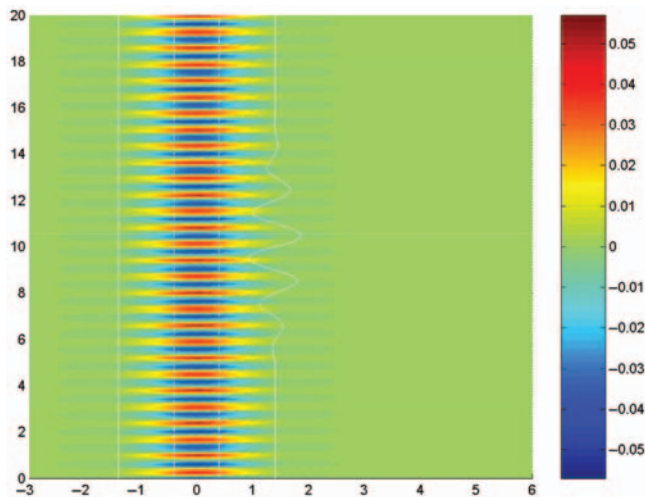


Figure 5. Real part of the near field of w_0 .

Table 1. Parameters of the waveguide.

n_{co}	n_{cl}	n_{ja}	k	R_{co}	$h = R_{\text{cl}}$	d^2
1.45	1.40	1.00	2π	0.4	1.4	43.52

375 The index of refraction is supposed to be piecewise constant. In particular n_{co} , n_{cl} and n_{ja} will denote the index of refraction of the core, cladding and jacket, respectively (Table 1).

380 We notice that there is no symmetry in the perturbation, but, thanks to the fact that the index of refraction is piecewise constant, it is possible to find a transformation Γ such that $n_\varepsilon(x, z)$ is mapped into $n_0(t)$, where $n_0(t)$ represents the index of refraction in the new coordinates (t, s) . We choose $S(s)$ and $T(t)$ as in Figure 3:

$$S(s) = A \left[1 - \left(\frac{s - s_0}{\omega} \right)^2 \right]^3 \sin(2\pi a_0 s) \chi_{(s_0 - \omega, s_0 + \omega)}(s), \quad (53)$$

and

$$T(t) = \left[1 - \left(\frac{t - R_{\text{cl}}}{\rho} \right)^2 \right]^3 \chi_{(R_{\text{cl}} - \rho, R_{\text{cl}} + \rho)}(t), \quad (54)$$

385 with $\rho = R_{\text{cl}} - R_{\text{co}}$ and where s_0 and ω are the centre and the half of the width of the perturbation, respectively. This choice of S and T amounts to a perturbation of the interface between cladding and jacket as in Figure 2.

The simulations presented here, refers to the following choices of a_0 : $a_0 = 0.5$ and $a_0 = 1.0$.

390 In Section 5.1 we describe how we obtain estimates for ε_0 (the maximum amplitude of the perturbation). In Sections 5.2 and 5.3 we study the behaviour of the solution in proximity of the waveguide (*near-field*) and far from that (*far-field*), respectively.

5.1. Computing ε_0

395 In this subsection we describe how we obtain an estimate for ε_0 . We notice that ε_0 depends on the the constants C_0 and K , where C_0 depends only on the weight function μ chosen and K depends also on the perturbation. We will calculate such constants for several choices of the weight function μ , and then evaluate the corresponding ε_0 . In particular, we will consider functions μ of the form

$$\mu(x, z) = \left(1 + \frac{|x - x_0|^2 + |z - z_0|^2}{\delta^2} \right)^{-m_1}, \quad (55)$$

400 where $P_0 \equiv (x_0, z_0)$ is the centre of the perturbation, and

$$\mu(x, z) = \mu_{a_1}(|x|) \mu_{a_2}(|z|), \quad (56)$$

Table 2. Bounds for ε_0 when μ is as in (55).

μ as in (55)							
(x_0, z_0)	B	m	a_0	ε_0	C_0	K	B_0
O	1	2	0.5	3.54e-5	7.54e+2	7.46e+3	2.82e+4
O	1	2	1.0	1.19e-5	7.54e+2	2.21e+4	8.36e+4
P_0	1	2	0.5	1.50e-3	7.54e+2	1.74e+2	6.58e+2
P_0	1	2	1.0	1.50e-3	7.54e+2	1.74e+2	6.58e+2
P_0	0.5	2	0.5	2.97e-3	1.11e+3	1.73e+2	3.36e+2
P_0	0.5	2	1.0	2.97e-3	1.11e+3	1.73e+2	3.36e+2
P_0	2	2	0.5	1.51e-3	7.66e+2	1.73e+2	6.60e+2
P_0	2	2	1.0	1.51e-3	7.66e+2	1.73e+2	6.60e+2
P_0	1	1.2	0.5	5.49e-2	1.29e+3	9.03	1.82e+1
P_0	1	1.2	1.0	3.53e-2	1.29e+3	14.05	2.83e+1

Table 3. Bounds for ε_0 when μ is as in (56).

μ as in (56)						
(x_0, z_0)	m	a_0	ε_0	C_0	K	B_0
P_0	1	0.5	5.72e-2	4.29e+3	5.91	1.75e+1
P_0	1	1.0	1.65e-2	4.29e+3	20.48	6.06e+1
P_0	0.4	0.5	5.70e-2	4.32e+3	5.91	1.75e+1
P_0	0.4	1.0	1.64e-2	4.32e+3	20.48	6.07e+1
P_0	2	0.5	5.51e-2	4.69e+3	5.91	1.81e+1
P_0	2	1.0	1.59e-2	4.69e+3	20.48	6.28e+1
P_0	2/3	0.5	5.73e-2	4.26e+3	5.91	1.74e+1
P_0	2/3	1.0	1.65e-2	4.26e+3	20.48	6.04e+1

where

$$\mu_{a_l}(t) = \begin{cases} 1, & 0 \leq t \leq a_l, \\ [1 + (t - a_l)^2]^{-m_2}, & t > a_l, \end{cases}$$

with $l=1, 2$, $m_1 > 1$, $m_2 > 0$ and where a_l , $l=1, 2$ is half of the side of P parallel to the x - and z -directions, respectively. All the results in [13 and 14] and the ones of the Section 4 can be easily generalized to such choices of μ .

Tables 2 and 3 show the resulting estimates for ε_0 .

5.2. Near-field

We show what happens near the perturbed zone of the waveguide represented in Figure 2. We will consider perturbations represented by the function in (53) corresponding to the values $a_0=0.5$ and $a_0=1.0$ and show the numerical results in Figures 6–8 and 9–10, respectively.

In Table 1, we report the values of the relevant parameters of the waveguides. With these parameters, the waveguide supports several guided modes; the first one corresponds to the values $\lambda_1^s = 3.3016$ and $\beta_1^s = 8.9276$.

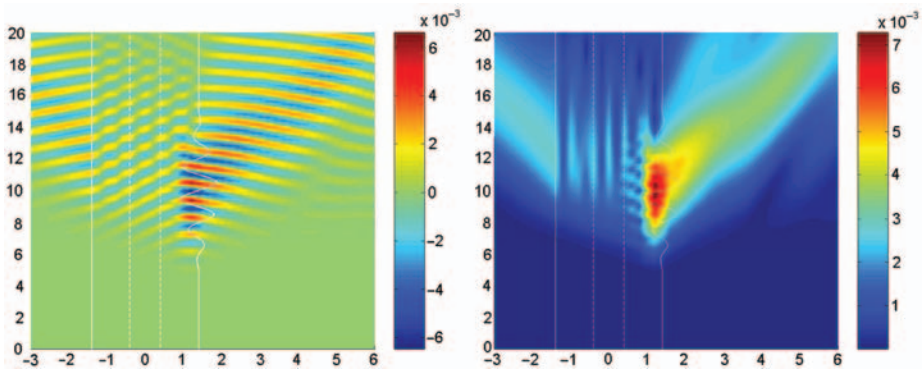


Figure 6. The two pictures show, respectively, the real part and the absolute value of w_1 for $a_0 = 0.5$.

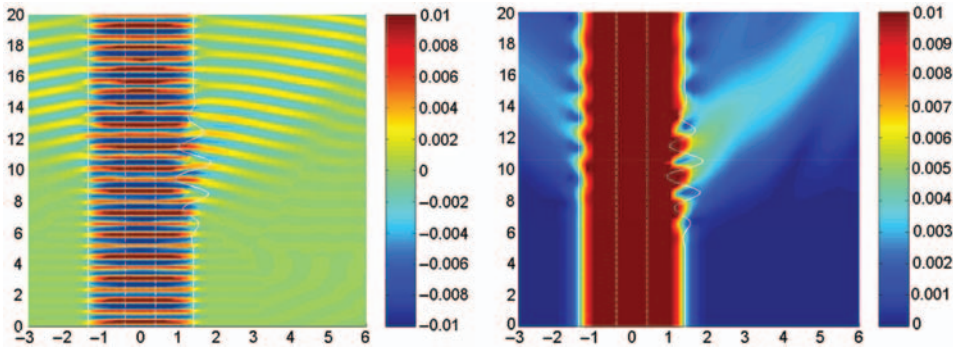


Figure 7. Real part and modulus of the near field of $w_0 + \epsilon w_1$ for $a_0 = 0.5$ with $\epsilon = 1$.

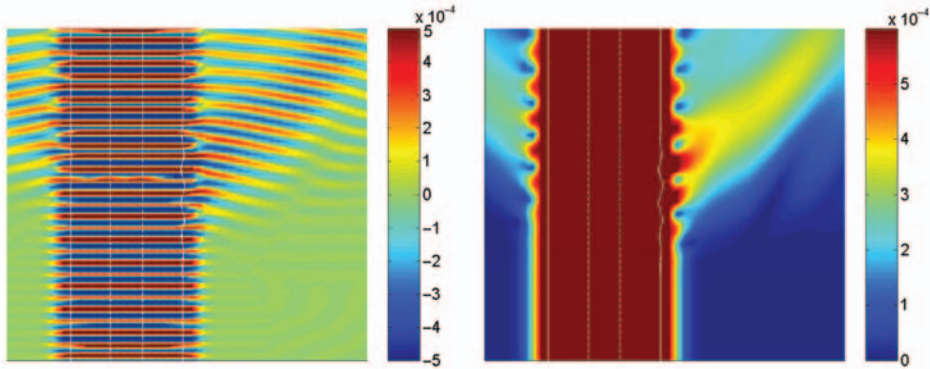


Figure 8. Real part and modulus of $w_0 + \epsilon w_1$, with $a_0 = 0.5$ and $\epsilon = 0.057$.

As already mentioned, we are interested in what happens to the wave propagation when a pure guided mode is propagating in the waveguide. Thus, we suppose that w_0 is the first forward propagating guided mode supported by the rectilinear waveguide (Figure 5):

$$w_0(t, s) = v_s(t, \lambda_1^s) e^{i\beta_1^s s},$$

420 with $\beta_1^s = \sqrt{k^2 n_*^2 - \lambda_1^s}$.

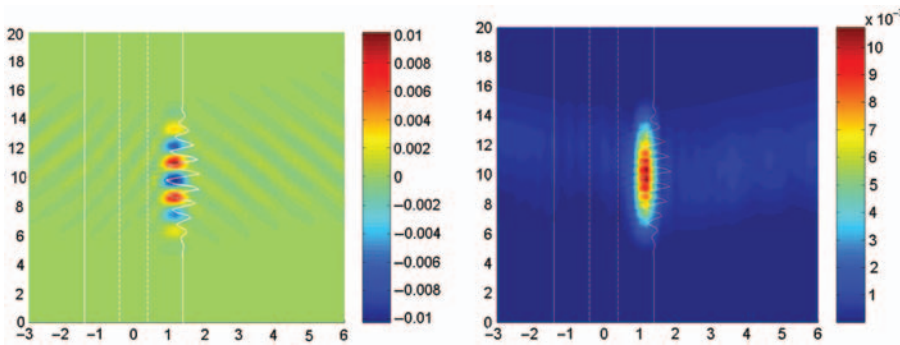


Figure 9. The two pictures show, respectively, the real part and the absolute value of w_1 for $a_0 = 1.0$.

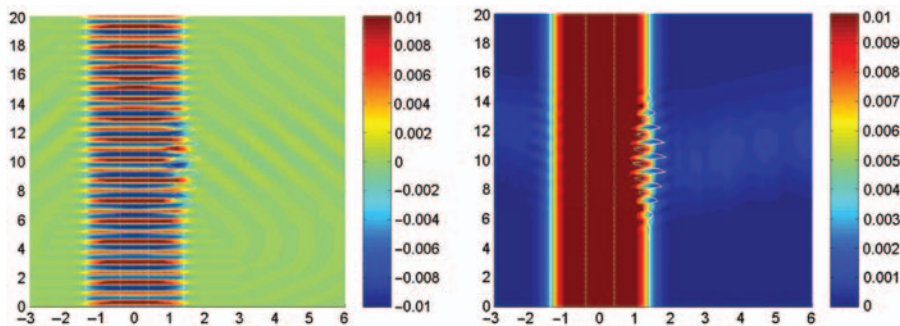


Figure 10. Real part and modulus of the near field of $w_0 + \varepsilon w_1$, for $a_0 = 1.0$.

In Figures 6 and 9 the real part and the modulus of w_1 are represented. To compute $w_1(t, s)$, i.e. the integral

$$w_1(t, s) = - \int_P G(t, s; t_1, s_1) L_1 w_0(t_1, s_1) dt_1 ds_1,$$

we use the trapezoidal rule on a rectangular grid in the (t, s) -plane (which corresponds to a ‘perturbed’ grid in the (x, z) -plane, as shown in Figure 4). The sampling intervals are chosen by dividing the perturbed zone P in 12×24 rectangles.

Now, we show how we computed the integrals defining G . Firstly, by changing the variables, we write G^r and G^e as

$$G^r = -i \sum_{j \in \{s, a\}} \int_0^{kn_{cl}} e^{i|z-\zeta|\mu} v_j(x, k^2 n_*^2 - \mu^2) v_j(\xi, k^2 n_*^2 - \mu^2) \sigma_j(k^2 n_*^2 - \mu^2) d\mu,$$

and

$$G^e = - \sum_{j \in \{s, a\}} \int_0^{+\infty} e^{-|z-\zeta|\mu} v_j(x, k^2 n_*^2 + \mu^2) v_j(\xi, k^2 n_*^2 + \mu^2) \sigma_j(k^2 n_*^2 + \mu^2) d\mu;$$

then we use the trapezoidal rule with sampling intervals of length $kn_{cl}/80$ in G^r and of $kn_*/40$ in G^e , where we truncate the integral at $\mu = kn_*$.

435 Figures 7 and 10 show $w_0 + \varepsilon w_1$ corresponding to the two different perturbations considered. Here we set $\varepsilon = 1$ in order to emphasize w_1 out. As already mentioned, our results hold for $\varepsilon \leq \varepsilon_0$, where $\varepsilon_0 = B_0^{-1}$ is given by (52). In Tables 2 and 3 we computed several estimates of ε_0 . Figure 8 shows the real part and the modulus of $w_0 + \varepsilon w_1$ with $\varepsilon = 0.057$ (the best estimate for ε_0 we obtained) for the case in which $a_0 = 0.5$.

440 We notice that in the first example, a small perturbation in the profile of the cladding determines a sort of plane wave going out from the waveguide. In the second example, the different shape (in frequency) of the perturbation does not create an important outgoing wave, but the intensity of w_1 is mostly confined in the region close to the perturbation.

445 We want to stress that Figures 6–10 represent the *near field* of the wave propagation. The computations in a wider region of the plane would require a large increase in terms of time and more appropriate quadrature formulas. This problem is due to the oscillatory behaviour of the functions defining G .

5.3. Far-field

450 As well as in the near field, we are interested in the behaviour of the *far-field*, which describes the behaviour of the solution far from the waveguide. A method for calculating a uniform asymptotic expansion of the far-field of the solution was proposed in [14]. Even if the far-field expansion was not computed explicitly, the following formulas follow easily from the results in [14]. Let u^{rad} be given by (13), then

$$u^{\text{rad}} \sim \frac{e^{i(Rkn_{\text{cl}} - \frac{3}{4}\pi)}}{\sqrt{R}} \Theta(\vartheta) + \mathcal{O}\left(\frac{1}{R}\right), \quad (57)$$

455 uniformly for $\vartheta \in [0, \pi/2]$, as $R \rightarrow +\infty$, where

$$\Theta(\vartheta) = \sqrt{\frac{kn_{\text{cl}}}{2\pi}} \sum_{j \in \{s, a\}} \sin \vartheta \sigma_j(\lambda_0(\vartheta)) \alpha_j(k^2 n_*^2 - \mu_0(\vartheta)^2) \hat{F}^j(\lambda_0(\vartheta), \mu_0(\vartheta)),$$

with

$$\alpha_j(\lambda) = \frac{e^{-ih\sqrt{\lambda-d^2}}}{2} \left[\phi_j(h, \lambda) + \frac{\phi_j'(h, \lambda)}{i\sqrt{\lambda-d^2}} \right],$$

$$\mu_0(\vartheta) = kn_{\text{cl}} \cos \vartheta, \quad \lambda_0(\vartheta) = k^2(n_*^2 - n_{\text{cl}}^2 \cos^2 \vartheta), \quad \beta_m^j = \sqrt{k^2 n_*^2 - \lambda_m^j},$$

460 and

$$F^j(\lambda, \zeta) = \int_{-\infty}^{+\infty} f(\xi, \zeta) v_j(\xi, \lambda) d\xi, \quad \hat{F}^j(\lambda, \mu) = \int_{-\infty}^{+\infty} F^j(\lambda, \zeta) e^{-i\zeta\mu} d\zeta.$$

465 Figure 11 shows the absolute value of the angular component of the far-field of u^{rad} as a function of the angular variable ϑ , with $\vartheta \in [0, \pi/2]$. The two pictures in Figure 11 correspond to the two cases described in the previous subsection. We notice that different kind of perturbations affect the far-field in a remarkable different way.

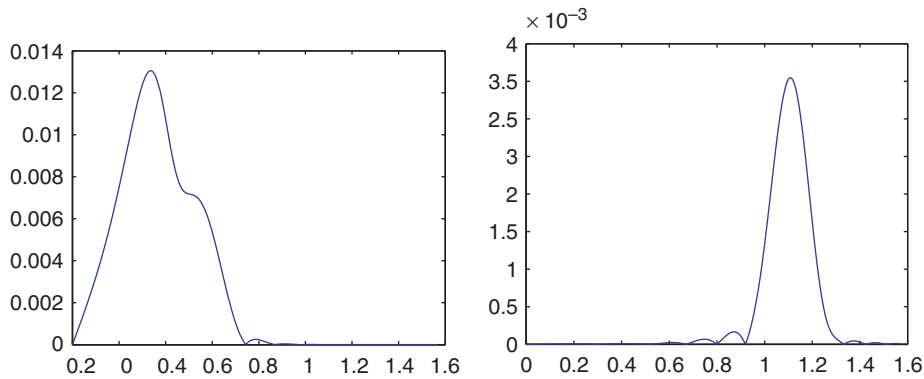


Figure 11. Absolute value of the angular component of the far-field as a function of the angular variable ϑ for $a_0 = 0.5$ and $a_0 = 1.0$, respectively.

Acknowledgements

470 This work has been partially supported by the PRIN project ‘Equazioni alle derivate parziali e
disuguaglianze funzionali: aspetti quantitativi, proprietà geometriche e qualitative, applicazioni’,
financed by MIUR. The author wish to thank Prof. Rolando Magnanini for his constant support in
writing this article. The author is also indebted to Prof. Fadil Santosa and Prof. Fernando Reitich,
who suggested several topics studied in this work while he was visiting the Institute for Mathematics
and its Applications (IMA) at University of Minnesota.

Note

- 475 1. Here and in the rest of the section, we use the following notation: by a subscript, as in $L_{\varepsilon}u$,
we denote functions of the variables (x, z) , whereas a superscript, as in $L^{\varepsilon}w$, indicates (the
corresponding) functions of the variables (t, s) .

References

- 480 [1] P.G. Dinesen and J.S. Hesthaven, *Fast and accurate modeling of waveguide grating couplers*,
J. Opt. Soc. Am. A 17 (2000), pp. 1565–1572.
[2] ———, *Fast and accurate modeling of waveguide grating couplers. II. The three-dimensional
vectorial case*, J. Opt. Soc. Am. A 18 (2001), pp. 2876–2885.
[3] J.S. Hesthaven, P.G. Dinesen, and J.P. Lynov, *Spectral collocation time-domain modeling of
diffractive optical elements*, J. Comp. Phys. 155 (1999), pp. 287–306.
485 [4] R. Horvath, L.C. Wilcox, H.C. Pedersen, N. Skiversen, J.S. Hesthaven, and P.M. Johansen,
*Analytical theory of grating couplers for waveguide sensing: A perturbational approach and its
limitations*, Appl. Phys. B: Lasers and Optics 81 (2005), pp. 65–73.
[5] L. Wilcox, P.G. Dinesen, and J.S. Hesthaven, *Fast and accurate boundary variation method for
multilayered diffraction optics*, J. Opt. Soc. Am. A 21 (2004), pp. 757–769.
490 [6] O.P. Bruno and F. Reitich, *Numerical solution of diffraction problems: a method of variation of
boundaries*, J. Opt. Soc. Am. A 10 (1993), pp. 1168–1175.
[7] ———, *Numerical solution of diffraction problems: a method of variation of boundaries. II. Finitely
conducting gratings, Pade approximants, and singularities*, J. Opt. Soc. Am. A 10 (1993),
pp. 2307–2316.
495 [8] ———, *Numerical solution of diffraction problems: a method of variation of boundaries. III doubly
periodic grating*, J. Opt. Soc. Am. A 10 (1993), pp. 2551–2563.

- [9] D.P. Nicholls and F. Reitich, *A new approach to analyticity of Dirichlet-Neumann operators*, Proc. R. Soc. Edinb., Sect. A, Math. 131 (2001), pp. 1411–1433.
- [10] ———, *Stability of high-order perturbative methods for the computation of Dirichlet-Neumann operators*, J. Comput. Phys. 170 (2001), pp. 276–298.
- [11] ———, *Analytic continuation of Dirichlet-Neumann operators*, Numer. Math. 94 (2003), pp. 107–146.
- [12] R. Magnanini and F. Santosa, *Wave propagation in a 2-D optical waveguide*, SIAM J. Appl. Math. 61 (2001), pp. 1237–1252.
- [13] G. Ciraolo and R. Magnanini, *Analytical results for 2-D non-rectilinear waveguides based on the Green's function*, to appear in Math. Meth. Appl. Sci.
- [14] G. Ciraolo and R. Magnanini, *A radiation condition for uniqueness in a wave propagation problem for 2-D open waveguides*, to appear in Math. Meth. Appl. Sci.
- [15] A.W. Snyder and D. Love, *Optical Waveguide Theory*, Chapman and Hall, London, 1974.
- [16] D. Gilbarg and N.S. Trudinger, *Elliptic Partial Differential Equations of Second Order*, Springer-Verlag, ■, 1983.
- [17] R.A. Adams and J.G. Fournier, *Sobolev Spaces*, Academic Press, ■, 2003.
- [18] D. Marcuse, *Light Transmission Optics*, Van Nostrand Reinhold Company, New York, 1982.

500

505

510

4

5

3